CrossMark

Investigation of the some physical properties of Ge-doped ZnO thin films deposited by thermionic vacuum arc technique

Reza Mohammadigharehbagh[1,2] · Soner Özen[1] · Hafizittin Hakan Yudar[1] · Suat Pat[1] ·
Şadan Korkmaz[1]

Abstract We exhibit the first nano-crystalline Ge–ZnO thin films deposited on glass and PET substrates by a thermionic vacuum arc technique. The effect of Ge doping on the structural, morphological and optical properties of ZnO:Ge films were investigated. An X-ray diffraction (XRD), atomic force microscopy, field emission scanning electron microscopy (FESEM) and UV–Vis spectrophotometer were used for the analysis. XRD patterns show the polycrystalline structure of the films in the range of 20°–80°. The roughness value for the ZnO:Ge on PET substrate was increased due to agglomeration of the grains. The results are in a good agreement with the FESEM images. Using Filmetrics F20 tool, the thickness values of the deposited thin films were obtained as 60 and 80 nm on glass and PET substrates, respectively. The optical properties of the films such as transmittance, absorbance, refractive index, and reflectance were determined. The band gap values were obtained as to be 3.43 and 3.38 eV glass and PET substrates, respectively. It was found that band gap variation of ZnO is very small with Ge doping.

1 Introduction

ZnO materials are very popular for their technological applications due to its excellent properties. The ZnO material is a wide band gap (~3.3 eV) material of the II–VI semiconductor group. ZnO material crystallizes in hexagonal wurtzite and cubic zincblende structure. Doped material changes the physical properties of the ZnO material. The doped ZnO material used in the numerous application fields in the technological world. These products are used in varistors, transparent high power electronics, optical waveguides, solar cells, UV light emitting apparatus, piezoelectric devices, laser diodes, thin film transistors, flat display panel and photoconductors fields and etc [1–4]. ZnO has unique and remarkable properties such as high electrochemical consistency, lack of toxicity, high transparency between in the range of the 400–700 nm. The material has a direct band of about 3.37 eV at room temperature as well as the high binding energy of 60 meV [5]. For doping of the ZnO material, carbon, gallium, boron, vanadium, aluminum and other have been represented in the literature [6–8].

ZnO and doped ZnO materials have been deposited by different type of synthesis methods such as radio frequency sputtering [9], molecular beam epitaxy [10], pulsed laser deposition [11], atomic layer deposition [12], direct current magnetron sputtering [13], sol–gel method [14], chemical spray pyrolysis [15], chemical vapor deposition [16], reactive evaporation, spin coating [17], metal organic chemical vapor deposition [18], electron beam evaporation, thermal oxidation [19] and etc.

According to the literature, Ge atom replacements the Zn sites in the ZnO crystal network. This replacement concentration can give rise to decrease in the semiconductor resistance sources by creating of two electrons [20]. On the other hand, small ionic radius value of the Ge ion (0.53 A) according to the Zn ion (0.74 A) is another advantage of easy replacement in the ZnO films. Thus, Ge-doped in the ZnO structure paved the way of employing of this material in the industrial applications until easily and prosperous

✉ Suat Pat
suatpat@ogu.edu.tr

1 Department of Physics, Eskişehir Osmangazi University, 26480 Eskişehir, Turkey

2 Department of Physics, Islamic Azad University, Urmia Branch, Urmia, Iran

substitution of the elements instead of Zn sites [21]. Ge element possesses an indirect band gap and its value is equal to 0.12 eV [22]. In the present research, the germanium doped ZnO (ZnO:Ge) thin films deposited using a thermionic vacuum arc (TVA) technique on glass and PET substrates. This is the first report on the ZnO:Ge films deposited by TVA method. Then, some physical properties such as the structural, morphological, surface and optical of films systematically were studied for the high-resolution analysis devices. The TVA technique has been made different advantages, such as fast deposition process, high purity, and high surface homogeneity of the deposited films.

2 Experimental details

In TVA technique, the pure arc plasma creates using anode and cathode. An electron gun as a cathode is used to evaporation of the material. As an anode, tungsten evaporation boat was used. Ge and ZnO particle were placed into evaporation boat. After the reach proper vapor pressure of the material, material plasma is created by high voltage. In the coating process, the vacuum chamber was pumped down to base pressure (5×10^{-5} Torr). The distance between anode and cathode was kept constant as to be 3–4 mm. This technique can work without any buffer or a noble gas. The deposition process and thickness of the films were monitored using the in-situ thin film thickness measurement apparatus. The main deposition procedure of TVA technique was reported in previous papers [6, 23, 24]. The parameters for the deposition procedure were listed in Table 1.

3 Results and discussion

Atomic force microscopy (AFM) measurements were done to evaluate the morphological and surface characteristics of the ZnO:Ge thin films on glass and PET substrates. Obtained two-dimension and three-dimension AFM images of the deposited films were exhibited in Fig. 1a–d. The AFM measurements (Ambios Q-scope) were done in the non contact mode. The surface parameters such as roughness,

Table 1 Deposition parameters of TVA technique

Samples	ZnO:Ge/Glass ZnO:Ge/PET
Discharge current (A)	0.5
Deposition time (s)	10
Working pressure (Torr)	7×10^{-5}
Applied voltage (V)	800
Filament current (A)	18.5

Fig. 1 Two dimensions AFM images of ZnO:Ge thin films deposited on **a** glass and **b** PET substrates, three dimensions AFM images of the films on **c** glass and **d** PET substrates, height distribution function of the films on **e** glass and **f** PET substrates, and FESEM images (50k× magnification) of the films coated on **g** glass and **h** PET substrate, respectively

peak–valley variation, skewness, kurtosis were also obtained by AFM device. All tests were performed in the room temperature situation. It is evident that surface properties such as roughness value play a crucial effect on the charge transfer capacity [25]. In addition, the height distribution histogram of the samples coated on glass and PET substrates were shown in Fig. 1e and 1f, respectively. The root mean square (RMS) roughness of the films evaluated by the below relation [26]:

$$R_{(RMS)} = \sqrt{\sum_{l=1}^{n} \left(H_l - H_a\right)^2 / N} \qquad (1)$$

where, H_l and N represented a height of each point and number of observed surface points, respectively. H_a is the mean of points present on the surface of the investigated films. As can be seen from Table 2, RMS values of the samples are different from each other's. A Supra 40VP field emission scanning electron microscopy (FESEM) was used for the surface imaging. Obtained images are shown in Fig. 1g, h. As can be seen in Fig. 1d, grains of dimensions are very small. These results are in a good agreement with the AFM images. According to EDX analyses results, Ge/Zn mol ratio for coated surfaces are 2.9 or 2.7 for coated glass or PET substrates, respectively.

X-ray diffraction (XRD) measurements were realized by Pan Analytical Empryan device for the investigation of the microstructural properties of deposited ZnO:Ge films on glass and PET substrates. XRD patterns are shown the polycrystalline structure of the deposited films in the range of 20°–80°. Figure 2 exhibits the obtained indexed XRD pattern. ZnO (100), ZnO (101), ZnO (102), ZnO (110) and ZnO (103) peaks were detected in XRD patterns. It was found that the peak positions of the crystal planes were shifted. Ge–O and Ge crystalline phases were detected in the XRD patterns. This results show that Ge atom substitute for Zn atoms in the ZnO crystal structure. These results are consistent with the present literature [27, 28].

The following relation used for calculation of the average crystallite size of the deposited samples. This equation is know as Debye–Scherrer equation [29]:

$$D = \frac{k\lambda}{\beta \cos\theta} \qquad (2)$$

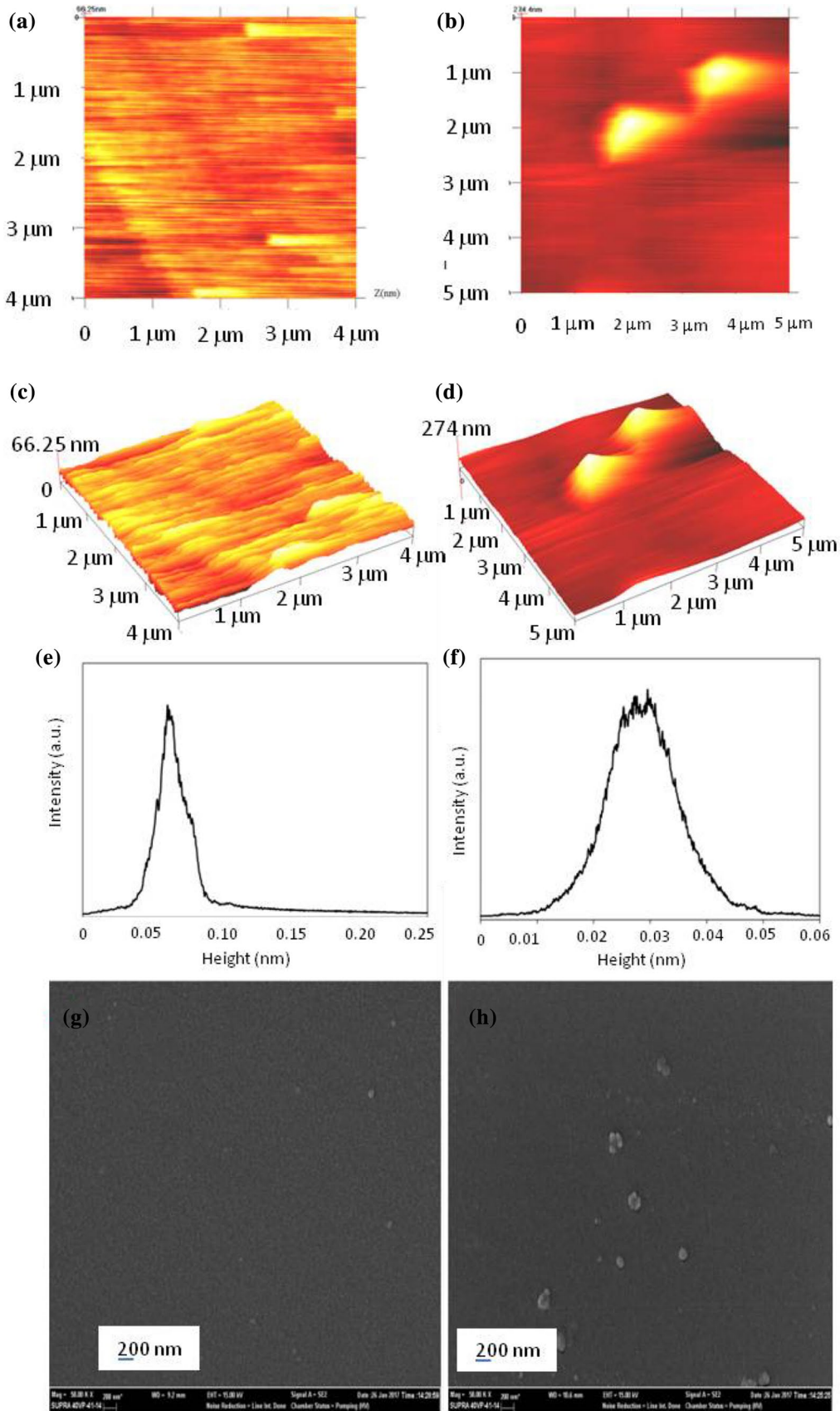where k is the shape factor (0.94), λ is X–ray wavelength (1.5406 A) and β is the expansion in the full width at half

Table 2 Surface characteristics of ZnO:Ge films on glass and PET substrates

Samples	RMS (nm)	Skewness (Ssk)	Kurtosis (Skr)
ZnO:Ge/glass	7	0.27	1.14
ZnO:Ge/PET	30	2.70	9.00

maximum (FWHM) in which calculated as radians, respectively. Moreover, θ is defined as the Bragg diffraction angle. Using the estimated average crystallite size values, the dislocation density (δ) and microstrain (ε) of the deposited thin films also evaluated with the Williamson and Smallman's relations;

$$\delta = \frac{1}{D^2} \tag{3}$$

$$\epsilon = \frac{\beta \cos \theta}{4} \tag{4}$$

and, in the same manner, the correlation between the lattice strain and FWHM of the films is given by:

$$\epsilon = \frac{\beta}{4 \tan \theta} \tag{5}$$

The dislocation density has been distinguished as dislocation lines in the volume of the films. The parameter was inferred as the crystal defect of deposited films. Furthermore, mismatch of the lattice at one end compared to another part of the samples strongly related to dislocation density value. It is concluded that obtained microstrain values of the films originate from dislocations, point defects such as site disorder, vacancies as well as other imperfections, which exist within the crystal structure. It is clearly that the value attributed to the growing conditions as well.

In addition, the number of crystallite per unit area (N) in terms of the thickness of films also expressed from the relation:

$$N = \frac{t}{D^3} \tag{6}$$

where, t stands for the thickness of the deposited samples. The calculated microstructural parameters of the deposited films are summarized in Table 3.
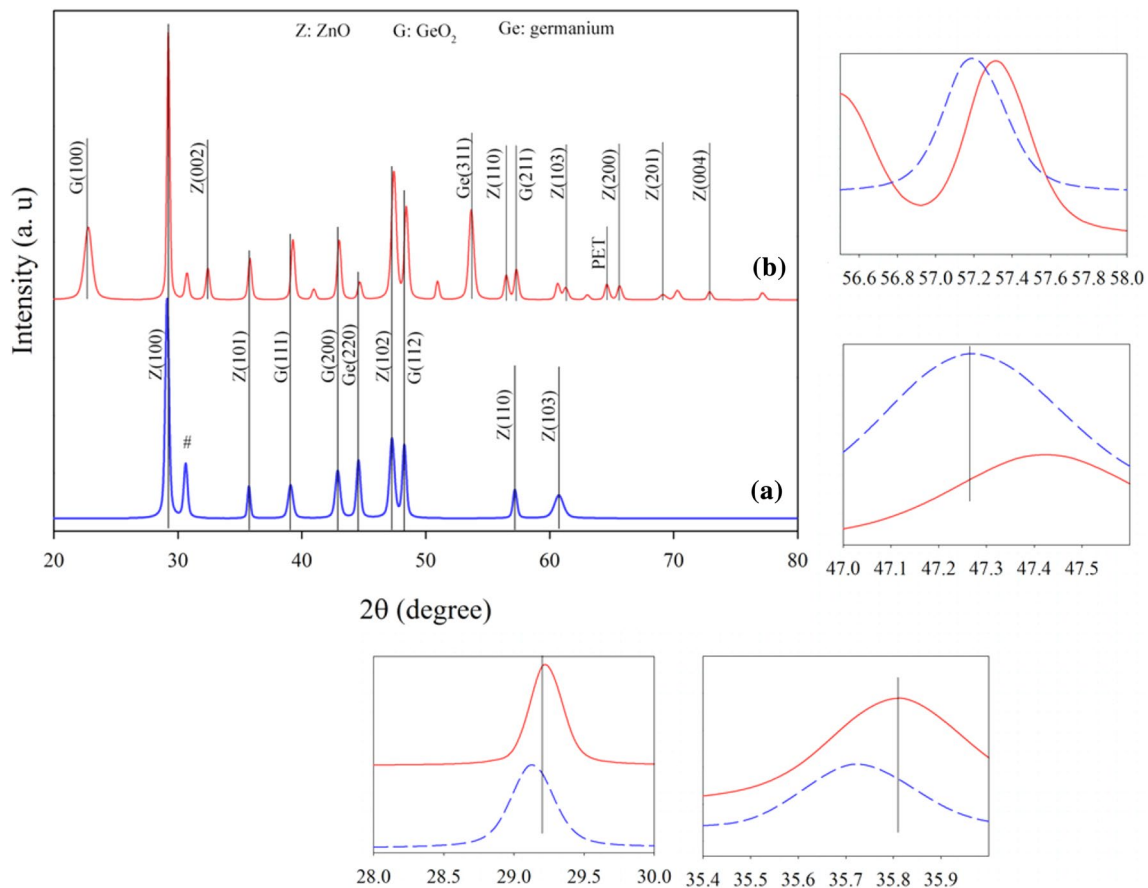

Fig. 2 XRD patterns of the ZnO: Ge deposited on (*a*) glass and (*b*) PET substrates. (Color figure online)

Table 3 Calculated XRD parameters for deposited Ge-doped ZnO samples on glass and PET substrate

	2θ (°)	Reflection plane	Phase	D (nm)	δ (m^{-2})×10^{15}	ε × 10^{-3}	∈ × 10^{-3}	NC (m^{-2}) ×10^{15}
ZnO:Ge films on glass substrate	29.70	(100)	ZnO	22	1.92	1.55	6.20	5.04
	35.71	(101)	ZnO	29	1.12	1.18	3.90	2.24
	39.07	(111)	GeO$_2$	18	2.85	1.88	5.60	9.11
	42.85	(200)	GeO$_2$	18	2.99	1.93	5.30	9.81
	47.26	(102)	ZnO	18	2.89	1.90	4.70	9.33
	48.31	(112)	GeO$_2$	22	2.03	1.59	3.90	5.49
	57.24	(110)	ZnO	23	1.88	1.53	3.20	4.88
	61.71	(103)	ZnO	10	8.60	3.28	6.50	47.8
ZnO:Ge films on PET substrate	22.80	(100)	GeO$_2$	11	8.14	3.19	16.1	58.8
	29.80	(100)	ZnO	25	1.54	1.39	5.50	4.85
	32.46	(002)	ZnO	22	1.93	1.55	5.60	6.80
	35.82	(101)	ZnO	24	1.63	1.43	4.60	5.29
	39.28	(111)	GeO$_2$	23	1.75	1.48	4.40	5.85
	42.96	(200)	GeO$_2$	22	2.01	1.58	4.30	7.21
	47.47	(102)	ZnO	18	3.03	1.94	4.80	13.3
	48.42	(112)	GeO$_2$	22	1.97	1.57	3.80	6.99
	56.50	(110)	ZnO	22.09	2.05	1.60	3.40	7.42
	57.34	(211)	GeO$_2$	22.81	1.92	1.55	3.20	6.74
	61.33	(103)	ZnO	8.30	14.5	4.26	8.40	140
	65.64	(200)	ZnO	22.08	2.05	1.60	3.00	7.43
	69.10	(201)	ZnO	15.66	4.08	2.26	4.00	20.8
	72.88	(004)	ZnO	22.58	1.96	1.57	2.60	6.95

Absorbance and transmittance graphs of the deposited films were measurement by Unico UV–Vis spectrophotometer in the range of 300–1000 nm. These graphs are seen in Fig. 3a, b.

The average transmittance values of the films were obtained as 90 and 80% on glass and PET substrates, respectively. The values demonstrate the higher transparency. The optical measurements for all samples were executed in the room temperature condition. Refractive indices and reflection graphs were determined by the Filmetrics F20 interferometer. These graphs are illustrated in Fig. 3c, d. These measurements are shown in the range of 400–1000 nm. The average refractive indices of the ZnO:Ge films were found as 1.85 and 1.81 for glass and PET substrates, respectively. In the same way, the reflectance values of the films reduce from 0.1 to 0.07 for glass and PET substrates, alternately. It can be seen from the refractive index, n, that the values decrease in terms of increasing wavelength for all samples [30].

The optical band gap of ZnO:Ge thin films deposited on glass and PET substrate can be determined by following equation;

$$\alpha h\nu = A\left(h\nu - E_g\right)^n \tag{7}$$

where A is a constant, h is the incident photon energy. α is the optical absorption coefficient and E_g represented as optical band gap of the deposited films. In the equation, n, refers the electronic transitions of the materials. The n can attain four different values, that is, 1/2, 2, 3/2 or 3. In this case, n is equal to 2 because of the indirect transition of the deposited thin films. The optical absorption coefficient of the samples calculated the following relation:

$$\alpha = \frac{1}{d} \ln\left(1/T\right) \tag{8}$$

herein, d and T are the thickness and transmittance in terms of the wavelength of the films, respectively. In the band gap plot, the optical band gap values can be determined by extrapolating the related direct lines downwards to the x-axis [31]. In the same way for all samples, the intersection of the direct lines can be specified the optical band values. The band gap values of the samples were founded as 3.43 and 3.38 eV for ZnO:Ge thin films coated on glass and PET substrates, respectively. The obtained values are consistent with values that reported by E.D. Gaspera and et al. [32]. The band gap graphs of the deposited films were shown in the Fig. 4. It is clear that there is a reverse relation between the thickness and band gap values in our results [33].
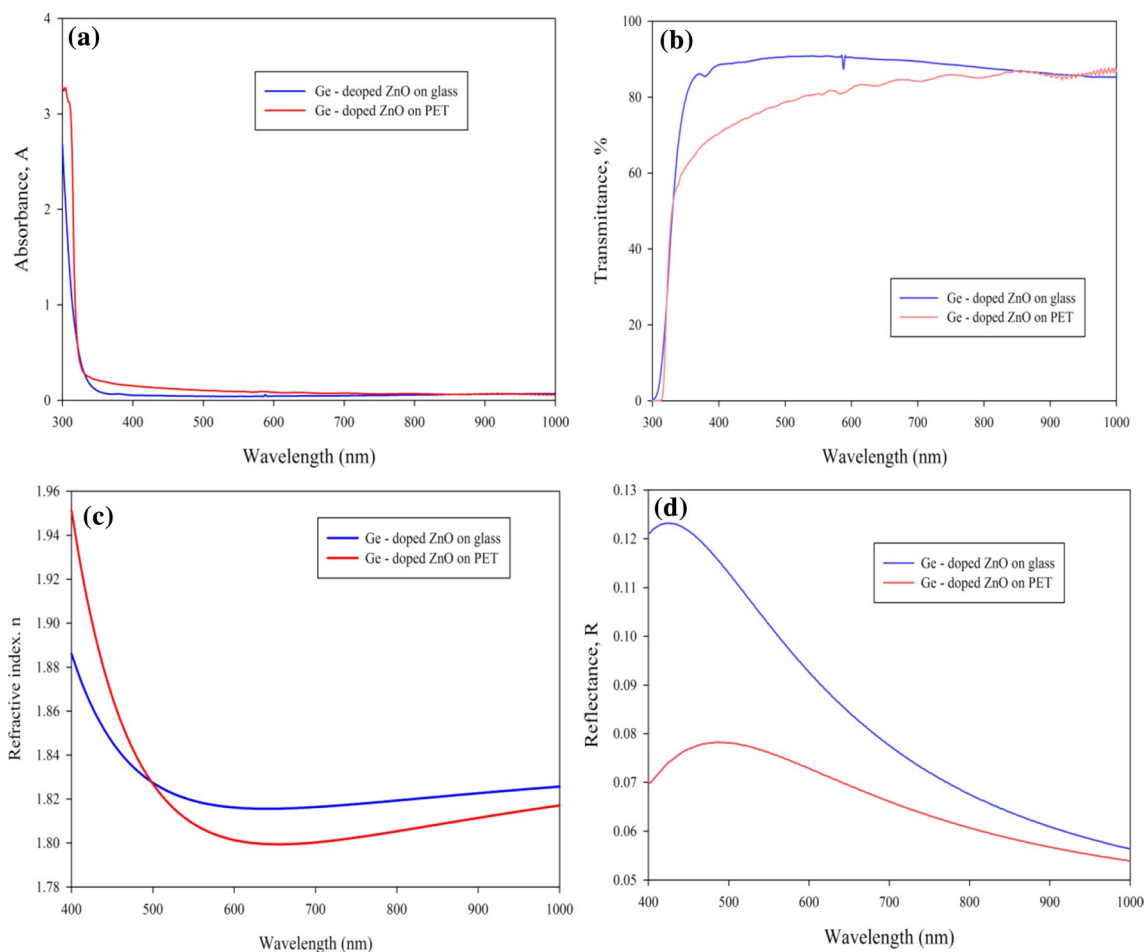
Fig. 3 **a** Absorbance, **b** transmittance, **c** refractive index and **d** reflectance graphs of the ZnO:Ge thin films deposited on glass and PET substrate, respectively. (Color figure online)
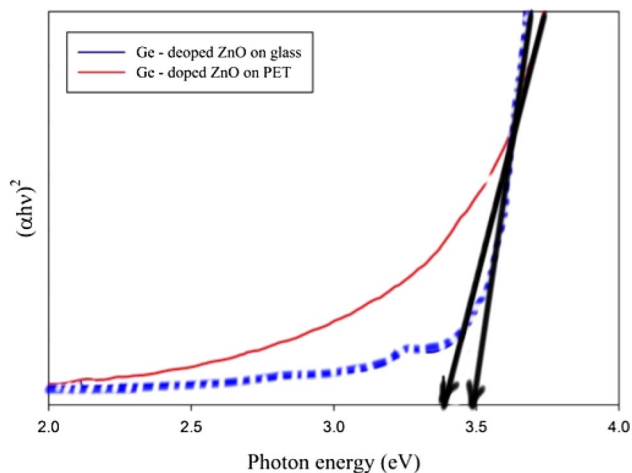

Fig. 4 Band gap graphs of the ZnO:Ge thin films deposited on glass and PET substrate, respectively. (Color figure online)

4 Conclusion

In this paper, the Ge-doped ZnO thin films successfully grown on glass and PET substrates using thermionic vacuum arc technique, for the first time. Some physical properties of films such as microstructural, morphological and optical properties were studied. Deposited films are in the polycrystalline structure according to the XRD patterns. The calculated average crystallite size of the films have been obtained between 10.79 and 29.92 nm for ZnO:Ge/glass and ZnO:Ge/PET samples, respectively. The thickness of the films recorded as 60 and 80 nm for the deposited films on glass and PET substrates, respectively. RMS values increase for films coated on PET substrates. According to the optical results, average transmittance values of the films defined as 90 and 80% on glass and PET substrates in the visible region, respectively. The optical band gaps of the samples were found as 3.43 and 3.38 eV for ZnO:Ge films coated on glass and PET substrates, respectively.

References

1. S. Pearton et al., Recent progress in processing and properties of ZnO. Prog. Mater. Sci. **50**(3), 293–340 (2005)
2. D.P. Norton et al., ZnO: growth, doping & processing. Mater. Today **7**(6), 34–40 (2004)
3. Z.-L. Tseng et al., Transparent Al-doped ZnO anodes in organic light-emitting diodes investigated using a hole-only device. Appl. Surf. Sci. **261**, 360–363 (2012)
4. Y. Wang et al., Electrical and structural properties of annealed ZnO:B thin films. J. Alloys Compd. **636**, 102–105 (2015)
5. Ü. Özgür et al., A comprehensive review of ZnO materials and devices. J. Appl. Phys. **98**(4), 11 (2005)
6. R. Mohammadigharehbagh et al., Investigation on the physical properties of C-doped ZnO thin films deposited by the thermionic vacuum arc. Eur. Phys. J. Plus **132**(1), 28 (2017)
7. N. Akin et al., Influence of RF power on the opto-electrical and structural properties of gallium-doped zinc oxide thin films. J. Mater. Sci. **28**(10), 7376–7384 (2017) [p. 1–9]
8. X. Meng et al., Optical and electrical properties of H and V co-doped ZnO films sputtered at room temperature. Optik-Int. J. Light Electron Optics **128**, 297–303 (2017)
9. V. Şenay et al., ZnO thin film synthesis by reactive radio frequency magnetron sputtering. Appl. Surf. Sci. **318**, 2–5 (2014)
10. A. Wierzbicka et al., Strain distribution in MgxZn1-xO layers with various content of Mg grown on a-plane sapphire by plasma-assisted molecular beam epitaxy. Appl. Surf. Sci. **404**, 28–33 (2017)
11. A. Krämer et al., ZnO thin films on single carbon fibres fabricated by pulsed laser deposition (PLD). Appl. Surf. Sci. **399**, 282–287 (2017)
12. M. Zafar, J.-Y. Yun, D.-H. Kim, Performance of inverted polymer solar cells with randomly oriented ZnO nanorods coupled with atomic layer deposited ZnO. Appl. Surf. Sci. **398**, 9–14 (2017)
13. T. Subramanyam, B. Srinivasulu Naidu, S. Uthanna, Physical properties of zinc oxide films prepared by dc reactive magnetron sputtering at different sputtering pressures. Cryst. Res. Technol. **35**(10), 1193–1202 (2000)
14. L.C.-K Liau, J.-S. Huang, Energy-level variations of Cu-doped ZnO fabricated through sol–gel processing. J. Alloys Compd. **702**, 153–160 (2017)
15. N. Tarwal, P. Patil, Superhydrophobic and transparent ZnO thin films synthesized by spray pyrolysis technique. Appl. Surf. Sci. **256**(24), 7451–7456 (2010)
16. P.-H. Lei, C.-H. Cheng, Fabrication of Ag nanoparticle/ZnO thin films using dual-plasma-enhanced metal-organic chemical vapor deposition (DPEMOCVD) system incorporated with photoreduction method and its application. Mater. Sci. Semicond. Process. **57**, 220–226 (2017)
17. B. Norris et al., Spin-coated zinc oxide transparent transistors. J. Phys. D **36**(20), L105 (2003)
18. C. Chandrakala et al., Synthesis, structure, vapour pressure and deposition of ZnO thin film by plasma assisted MOCVD technique using a novel precursor bis[(pentylnitrilomethylidine)(pentylnitrilomethylidine-µ-phenalato)]dizinc(II). J. Mol. Struct. **1130**, 1–9 (2017)
19. Y. Wang et al., Photoluminescence study of ZnO films prepared by thermal oxidation of Zn metallic films in air. J. Appl. Phys. **94**(1), 354–358 (2003)
20. D. Kim et al., Effect of oxygen pressure on electrical properties of Ge-doped ZnO thin films grown by using pulsed laser deposition. J. Korean Phys. Soc. **61**(6), 920–923 (2012)
21. M. Arita, M. Yamaguchi, M. Masuda, Electrical and optical properties of germanium-doped zinc oxide thin films. Mater. Trans. **45**(11), 3180–3183 (2004)
22. D.H. Fan, Z.Y. Ning, M.F. Jiang, Characteristics and luminescence of Ge doped ZnO films prepared by alternate radio frequency magnetron sputtering. Appl. Surf. Sci. **245**(1–4), 414–419 (2005)
23. V. Şenay et al., Optical, morphological and mechanical properties of an Al–Al2O3 nanocomposite thin film grown by thermionic vacuum arc. Optik-Int. J. Light Electron Optics **127**(6), 3383–3387 (2016)
24. S. Pat et al., GaN thin film deposition on glass and PET substrates by thermionic vacuum arc (TVA). Mater. Chem. Phys. **159**, 1–5 (2015)
25. C.O. Avellaneda, M.A. Berton, L.O. Bulhões, Optical and electrochemical properties of CeO 2 thin film prepared by an alkoxide route. Sol. Energy Mater. Sol. Cells **92**(2), 240–244 (2008)
26. J. Mazloom, F. Ghodsi, M. Gholami, Fiber-like stripe ATO (SnO2:Sb) nanostructured thin films grown by sol–gel method: optical, topographical and electrical properties. J. Alloys Compd. **579**, 384–393 (2013)
27. Y. Yu et al., Optical characteristics of Ge doped ZnO compound. J. Eur. Ceram. Soc. **24**(6), 1865–1868 (2004)
28. T. Zheng et al., Transitions of microstructure and photoluminescence properties of the Ge/ZnO multilayer films in certain annealing temperature region. Appl. Surf. Sci. **252**(24), 8482–8486 (2006)
29. Cullity, B., Structure of polycrystalline aggregates. Elements of X-ray Diffraction, (1978), p. 284.
30. S. Xue et al., Effects of post-thermal annealing on the optical constants of ZnO thin film. J. Alloys Compd. **448**(1), 21–26 (2008)
31. Ş. Korkmaz et al., Morphology, composition, structure and optical properties of CuO/Cu2O thin films prepared by RF sputtering method. Vacuum **131**, 142–146 (2016)
32. E. Della Gaspera et al., Plasmonic Ge-doped ZnO nanocrystals. Chem. Commun. **51**(62), 12369–12372 (2015)
33. S. Pati, Highly textured ZnO thin films grown using sol-gel route for gas sensing application. J. Alloys Compd. **695**, 3552–3558 (2017)